



## OPEN ACCESS

## EDITED BY

Yi-Xiang Chen,  
University of Science and Technology of  
China, China

## REVIEWED BY

Gengxin Deng,  
University of Science and Technology of  
China, China  
Zhen-Xin Li,  
University of Science and Technology of  
China, China  
Xiaochi Liu,  
Institute of Geology and Geophysics  
(CAS), China

## \*CORRESPONDENCE

Li-E. Gao,  
✉ liegao09@163.com

## SPECIALTY SECTION

This article was submitted to Petrology,  
a section of the journal  
Frontiers in Earth Science

RECEIVED 14 November 2022

ACCEPTED 13 December 2022

PUBLISHED 30 January 2023

## CITATION

Gao L-E, Zeng L, Yan L, Zhao L and  
Wang Y (2023), Structural changes in  
silicate melt: A record from high-field  
strength elements in the Himalayan  
Cenozoic leucogranites.  
*Front. Earth Sci.* 10:1097537.  
doi: 10.3389/feart.2022.1097537

## COPYRIGHT

© 2023 Gao, Zeng, Yan, Zhao and Wang.  
This is an open-access article  
distributed under the terms of the  
[Creative Commons Attribution License  
\(CC BY\)](https://creativecommons.org/licenses/by/4.0/). The use, distribution or  
reproduction in other forums is  
permitted, provided the original  
author(s) and the copyright owner(s) are  
credited and that the original  
publication in this journal is cited, in  
accordance with accepted academic  
practice. No use, distribution or  
reproduction is permitted which does  
not comply with these terms.

# Structural changes in silicate melt: A record from high-field strength elements in the Himalayan Cenozoic leucogranites

Li-E. Gao<sup>1\*</sup>, Lingsen Zeng<sup>1</sup>, Lilong Yan<sup>1</sup>, Linghao Zhao<sup>2</sup> and Yaying Wang<sup>1</sup>

<sup>1</sup>Institute of Geology, Chinese Academy of Geological Sciences, Beijing, China, <sup>2</sup>National Research Center for Geoanalysis, Chinese Academy of Geological Sciences, Beijing, China

Most Himalayan Cenozoic leucogranites are peraluminous magmas that have experienced various degrees of fractional crystallization. These leucogranites are characterized by relatively high degrees of heterogeneity in their elemental compositions. As the melt's Zr/Hf ratio passes ~20, there is an apparent change from positive to negative in the correlation between Zr (or Hf) and Zr/Hf ratio. As Nb/Ta ratio passes ~5, Nb first decreases and then increases, but Ta first slowly increases and then drastically increases. Such systematic geochemical variations are related to changes in the dissolution behavior of key accessory phases, which are the consequence of silicate melt structural changes associated with fractional crystallization and. As a granitic magma evolves, changes in the melt structure as shown by changes in the compositional parameters (e.g., NBO/T, A/CNK, and M/F) as well as in Zr/Hf and Nb/Ta ratios. When the melt's Zr/Hf and Nb/Ta ratio passes 20 and 5, respectively, NBO/T, M/F, and A/CNK first decrease and then increase; A/NK and C/NK first decrease and then become nearly constant; Na/K first becomes nearly constant and then increases. Moreover, a substantial change in the melt structure leads to a decrease in granitic viscosity, which in turn fractional crystallization of the granitic melts. Finally, such changes result in the mineralization of economically relevant rare elements in the Himalayan Cenozoic leucogranites.

## KEYWORDS

structural changes, silicate melt, high-field strength elements, leucogranites, Himalayan orogenic belt

## 1 Introduction

The structure of magma melt is an intrinsic property of the magma and is an important research Frontier in magmatic petrology and magma thermodynamics (Mo, 1985). Regardless of whether magma is primary or derived, it has a specific melt structure (Hou et al., 1992). The structure of magma melt has a significant impact on the

thermodynamic properties and physical properties of the magmatic system (such as density and viscosity), thereby affecting related dynamic processes of magma (such as crystallization, rising speed, diffusion, and distribution of elements) (Mysen, 1983; Mo, 1985; Bottinga et al., 1996; Losq et al., 2021). Changes in magma composition, temperature, and pressure are accompanied by changes in the melt structure, which inevitably lead to changes in the physical and chemical properties of the melt (Zhu and Zhang, 1996). Therefore, the structure of silicate melts provides a basis for understanding the relations between their structure and their physical, chemical, and thermal properties. The structure of silicate melts also aids in determining the conditions of the formation and evolution of magma on the Earth and other terrestrial planets (Mysen, 1983). In addition, research on the structure of silicate melts is not only limited to the field of geosciences but is also important for other fields, such as physics, materials science, electronic technology, chemistry, and metallurgy. Therefore, the significance of studying the structure of silicate melt cannot be overemphasized.

In the 1980's and 1990's, a group of scholars conducted in-depth studies on the melt structure of magma and asserted that the melt structure is restricted by its composition (Mysen et al., 1980; Mysen et al., 1982; Mo, 1985; Chen and Gao, 1986; Zhu and Zhang, 1996). Rather than relying on the properties of magma melts to infer their structure, the melt structure of magma can be determined directly by geochemical parameters. Mysen et al. (1980) proposed a structure model: NBO/Si (or NBO/T), i.e., the ratio of non-bridging oxygen (NBO) atoms to silicon (Si) atoms. However, when applied to peraluminous granites, NBO/Si comes out as negative. Therefore, Chen and Gao (1986) considered the structural role of aluminum (Al) and the existence of the volatile components, such as water (H<sub>2</sub>O) and fluorine, and revived the model. There is another parameter namely M/F, i.e., the ratio of network formers (F) to network modifiers (M), which reflects the degree of magma polymerization (Hou et al., 1992). Similarly, aluminum play a network formers role, but alkali elements play a network modifier role. An increase in the Al/(Na+K) ratio of aluminosilicate melts strongly affect melt polymerization and properties (Dickenson and Hess, 1982). Therefore, A/CNK, A/NK, C/NK, and Na/K can be used as indicators of melt structure (Dickenson and Hess, 1982; Linnen and Keppler, 1997; Losq et al., 2021). The Miocene granites found along the Himalayan orogenic belt have been considered to be peraluminous granites derived from crustal anatexis (Patiño Douce and Harris, 1998; Weinberg and Hasalove, 2015; Wu et al., 2015; Zeng and Gao, 2017). The leucogranites consist of two-mica granite, garnet-bearing leucogranite, and tourmaline-bearing leucogranite and are characterized by relatively high degrees of heterogeneity in their elemental (Ca, Na, K, Rb, Sr, Ba, Zr, Hf, Nb, Ta, Th, rare Earth elements) and radiogenic isotope (Sr, Nd, and Hf) compositions (Gao et al., 2017 and references therein). The systematic geochemical variations imply that the three types of leucogranite are cogenetic and that the two-mica

granite represents the more primary melt, whereas other leucogranites could be more evolved melts (Gao et al., 2021a). Gao et al. (2021a) suggested that fractional crystallization induces substantial changes in the melt structure and in turn a major change in the dissolution behavior of accessory phases and the geochemistry of key trace elements. Key questions in this regard are: Is structural change in the silicate melt widespread during the evolution of granite magma? Which geochemical parameters can help to characterize the change in the melt structure? How does change in the melt's structure affect the dissolution behavior of important accessory minerals (zircon, monazite), key major elements (Al, K, Na), and trace elements (Nb, Ta, Zr, Hf)? The structure change in silicate melt is therefore a subject of intensive research. As structural data become available, a system based on the structure may be developed for the prediction of important properties of magmatic systems.

## 2 Geological setting

From north to south, the Himalayan orogenic belt consists of Tethyan Himalaya, High Himalaya, Lesser Himalaya, and Sub-Himalaya, which are separated by the Southern Tibetan Detachment System (STDS), Main Central Thrust (MCT), and Main Boundary Thrust (MBT), respectively (Figure 1). The Cenozoic leucogranites along the Himalayan orogenic belt are distributed along the Tethyan Himalaya and the High Himalaya. Within the Tethyan Himalaya, from west to east, there are a series of well-defined gneiss domes, including Malashan, Xiaru, Lhagoi Kangri, Mabja, Sakya, Kangmar, Kampa, Ramba, and Yardoi. Each gneiss dome shares similar overall characteristics. They consist of deformed Paleozoic granitic gneisses and intermediate-grade metamorphic rocks. Additionally, they are intruded by Cenozoic granites in the core (Zhang et al., 2004; King et al., 2011; Zeng et al., 2011; Gao and Zeng, 2014; Liu et al., 2014; Gao et al., 2019), which are in turn overlain by low-grade metamorphic or un-metamorphosed sedimentary rocks of the Tethyan Himalaya Sequence (THS, Zhang et al., 2012). In the High Himalaya, the Cenozoic granitic rocks directly intrude into STDS or the High Himalayan Crystalline Sequence (HHCS), which comprises Proterozoic to early Paleozoic medium to high-grade metamorphic rocks (Hodges, 2000; Aikman et al., 2008; Wang et al., 2017). Available data show that the Miocene granitic rocks in the Tethyan Himalaya and High Himalaya have similar mineral compositions, crystallization ages, geochemical characteristics, and formation mechanisms (Zhang et al., 2004; Gao et al., 2017; Liu et al., 2019).

In this investigation, we summarize our published data on the whole-rock geochemistry of Miocene granitic rocks from the gneiss dome of Borong (Gao et al., 2021a) and Nariyongcuo (Gao et al., 2019) within the Tethyan Himalaya, as well as Gyirong (Gao et al., 2017), Yadong (Gao et al., 2021b) and Cona (Supplementary Table A1) regions along the High Himalaya

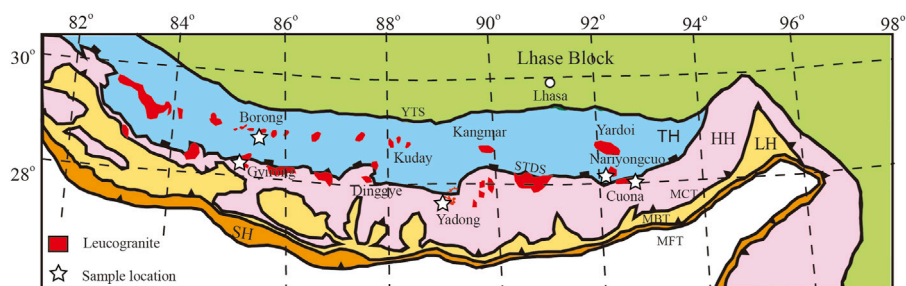


**FIGURE 1**

A simplified geologic map of the Himalayan orogenic belt. TH, Tethyan Himalaya; HH, High Himalaya; LH, Lesser Himalaya; SH, Sub-Himalaya; YZS, Yarlung Zangbo Suture Zone; STDS, Southern Tibetan Detachment System; MCT, Main Central Thrust; MBT, Main Boundary Thrust; MFT, Main Frontal Thrust.

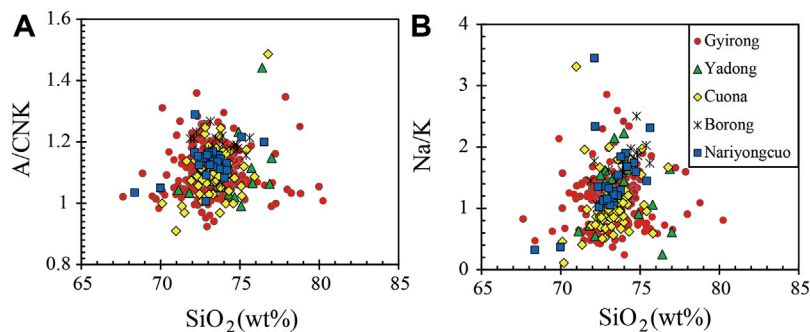


**FIGURE 2**

Major elemental characteristics of the Himalayan Miocene leucogranites.

as shown in Figure 1. The Borong Gneiss Dome is located in the western part of the Tethyan Himalaya and consists of various types of leucogranite in the core surrounded by mica-schist, marble, and quartzite toward the margin. Leucogranites include coarse-grained two-mica granite, garnet-bearing leucogranite, and sheared grayish two-mica granite. The Nariyongcuo Gneiss Dome, located to eastern Tethyan Himalaya, consists of many types of granites, containing two-mica granite, foliated leucogranites, and garnet-bearing leucogranite. Gyirong region located in the west of the High Himalaya. Some undeformed and foliated leucogranites intruding into STDS, as well as many undeformed leucogranites as dikes, veins and lenses intruded into HHCS. Leucogranites include two-mica granite, tourmaline-bearing leucogranite, and garnet-bearing leucogranite. Yadong region, located in the middle of the High Himalaya, consist of 23 Ma Gaowu tourmaline-bearing leucogranite emplaced within the very-low-grade THS and STDS, 20–18 Ma undeformed Dingga two-mica granite and 17–16 Ma two-mica granite intruded into both the HHCS and the overlying STDS (Liu et al., 2019). The Cona region located in the eastern

Himalayan orogenic belt. Undeformed granitic plutons, dykes or sills intruded into the HHCS. Leucogranites include two-mica granite, tourmaline-bearing leucogranite, and garnet-bearing leucogranite. North-South Trending Rift Zone vertically cut across above regions. These granites provide an important opportunity to study structural changes in the silicate melt.

### 3 Data and results

Most granites have high  $\text{SiO}_2$  (70.0–80.2 wt%), and their A/CNK ratios are greater than 1.0, showing that these granites are peraluminous high-silica magmas (Figure 2A). Na/K ratios are highly variable with  $\text{Na/K} = .2\text{--}3.4$  (Figure 2B). The concentrations and ratios of high-field strength elements are variable (Figure 3). For instance,  $\text{Zr} = 2.7\text{--}197$ ,  $\text{Hf} = .1\text{--}14.0$ ,  $\text{Nb} = 1.2\text{--}49.6$ ,  $\text{Ta} = .1\text{--}45.3$ . Zr/Hf ratios range from 7.6 to 40.6, and Nb/Ta ratios range from .9 to 18.0. As the melt's Zr/Hf ratio passes approximately 20, a decrease in Zr/Hf ratio is observed with a change in Zr (or Hf) (first

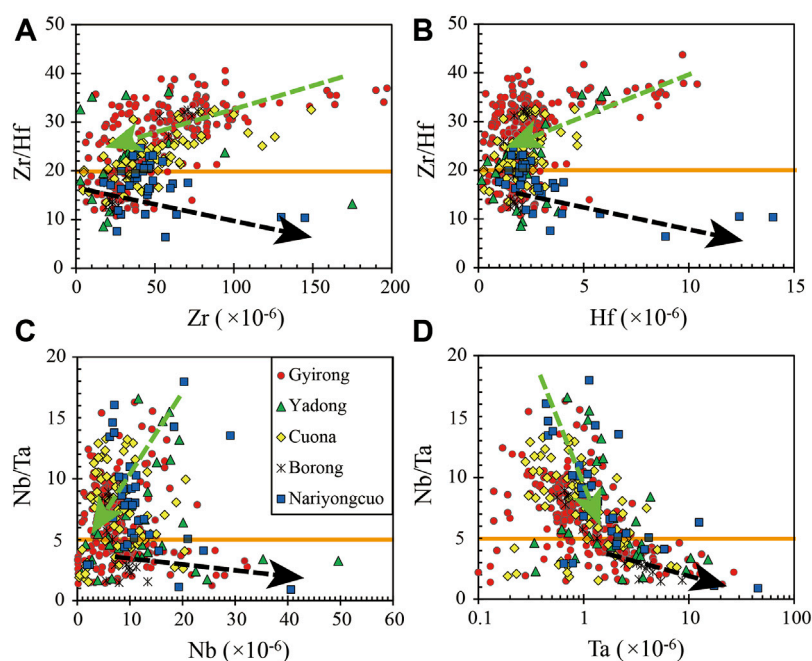


**FIGURE 3**

Systematic relationship between high-field strength elemental concentrations and ratios in the silica magmas. (A) Zr-Zr/Hf, (B) Hf-Zr/Hf, (C) Nb-Nb/Ta, (D) Ta-Nb/Ta.

decrease followed by increase; Figures 3A,B). Similar to Zr-Hf, when the melt's Nb/Ta ratio passes approximately 5, the relationships between Nb (or Ta) and Nb/Ta ratios also change. As Nb/Ta ratio decreases, Nb first decreases and then increases (Figure 3C). However, Ta first slowly increases and then drastically increases (Figure 3D).

The melt structure is represented by geochemical parameters with ratios of NBO/T, M/F, A/CNK, A/NK, C/NK, and Na/K. When the melt's Zr/Hf ratio passes 20, the melt structure changes as shown by the changes in the geochemical proxies of the melt's structure. As Zr/Hf ratio decreases, NBO/T, M/F, and A/CNK first decrease and then increase (Figure 4); A/NK and C/NK first decrease and then become nearly constant (Figure 5), while Na/K is at first nearly constant and then increases (Figure 5E). Similar to Zr-Hf, when the melt's Nb/Ta ratio passes 5, the melt structure changes. There is a similar relationship between geochemical parameters and Nb/Ta ratio (Figures 4, 5). Based on the Zr and LREE concentrations, granites with Zr/Hf and Nb/Ta ratio greater than 20 and 5, respectively, they yield lower temperatures inferred by zircon saturation thermometry ( $T_{Zr}$ , Watson and Harrison, 1983; Crisp and Berry, 2022) than those as by monazite saturation thermometry ( $T_{LREE}$ , Montel, 1993). However, they yield similar temperatures in the granites with Zr/Hf ratio less than 20 and Nb/Ta ratio less than 5, respectively (Figure 6).

## 4 Discussion

### 4.1 Behavior of high-field strength elements during magma evolution

Zr, Hf, Nb, and Ta are important high-field strength elements. Zr and Hf, as well as Nb and Ta, have the same charge, and similar ionic radiuses and are considered to be "geochemical twins." They have similar geochemical properties and are generally not be fractionated in most geological processes. However, Zr/Hf ratios and Nb/Ta ratios are variable, particularly in granites. Studies have demonstrated that Zr/Hf ratios and Nb/Ta ratios decrease in granites during their differentiation (Linnen and Keppler, 1997, 2002; Stepanov et al., 2013; Stepanov et al., 2014) or during interaction with late-stage magmatic fluids (Dostal et al., 2015; Ballour et al., 2016).

Zr-Zr/Hf and Hf-Zr/Hf systematic relationships are complex in the Himalayan Miocene leucogranites. In the high-silica peraluminous magma, when the melt's Zr/Hf ratio passes approximately 20, there is an apparent change from positive to negative correlation between Zr (or Hf) and Zr/Hf ratio (Figures 3A,B). The occurrence of Hf-rich zircon and a strong decrease in the Zr/Hf ratio in many highly peraluminous granites have been explained by crystal fractionation (Linnen and Keppler, 2002; Liu et al., 2019; Gao et al., 2021a). Zr and Hf are compatible in zircon, and zircon preferentially incorporates

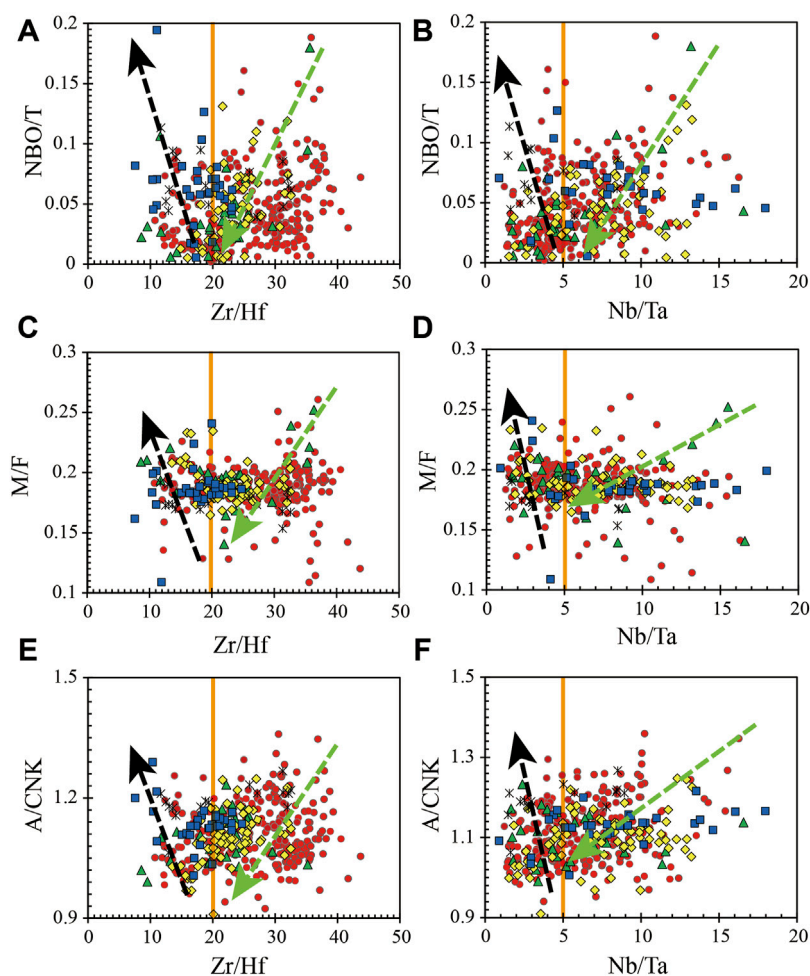


**FIGURE 4**

Relationship between the textural change in the silica melts (represented by NBO/T, M/F, and A/CNK) and high-field strength elements' ratios (Zr/Hf and Nb/Ta). NBO/T is the ratio of non-bridging oxygen (NBO) atoms to silicon (Si) atoms.  $NBO/T = (2 \times A - 4 \times T)/T$ , where  $A = O^{2-} + H_2O + F, T = Si + Ti + P + S + M_N^{3+}$  (if  $\Sigma M^{3+} > \Sigma M^{2+} + 2\Sigma M^{2+}$ ,  $\Sigma M_N^{3+} = \Sigma M^{3+} + 2\Sigma M^{2+}$ ; if  $\Sigma M^{3+} < \Sigma M^{2+} + 2\Sigma M^{2+}$ ,  $\Sigma M_N^{3+} = \Sigma M^{3+}$ ). M/F is the ratio of network formers (F) to network modifiers (M).  $M/F = [2 \times (Na_2O + K_2O) + CaO + MgO + FeO]/[2 \times TiO_2 + SiO_2 + Al_2O_3 + Fe_2O_3]$ .  $A/CNK = Al_2O_3/(CaO + Na_2O + K_2O)$ .

Zr over Hf. The fractional crystallization of zircon tends to decrease Zr/Hf in the residual melt. Consequently, the positive correlation between Zr (or Hf) and Zr/Hf imply fractional crystallization of zircon. However, as the melt's Zr/Hf ratio passes approximately 20, Zr and Hf start to increase, and a negative correlation exists between Zr (or Hf) and Zr/Hf ratio (Figures 3A,B). Based on zircon saturation thermometry and monazite saturation thermometry, the temperatures in the granites with Zr/Hf less than 20 are substantially lower than those with Zr/Hf greater than 20. Generally, zircon solubilities should decrease as temperature drops. Therefore, previous studies have suggested that changes in the melt structure affect mineral solubilities as granitic magma evolves into high-silica magma ( $SiO_2 > 74.0$  wt%, Linnen and Keppler, 2002; Guo et al., 2017; Zeng and Gao, 2017; Gao et al., 2021a). This model

could also explain the occurrence of Hf-rich zircon in the Himalayas in highly fractionated peraluminous granites (Liu et al., 2019). In the granites with Zr/Hf ratio greater than 20,  $T_{Zr}$  is lower than  $T_{LREE}$ , whereas the two thermometers yield similar temperatures in the granites with a Zr/Hf ratio less than 20 (Figure 6). Such a pattern implies that zircon solubilities increase as magmas evolve into high-silica peraluminous granites with Zr/Hf ratio less than 20, which also should be due to changes in the melt structure. Therefore, not only zircon fractional crystallization but also changes in the melt structure could lead to systematic variations in Zr and Hf and their ratio.

Both Nb and Ta are generally highly incompatible lithophilic elements in magmatic systems, where Ta is even less soluble than Nb (Zaraisky et al., 2010). However, there are a few accessory phases (such as titanite and rutile), which strongly concentrate on Nb and

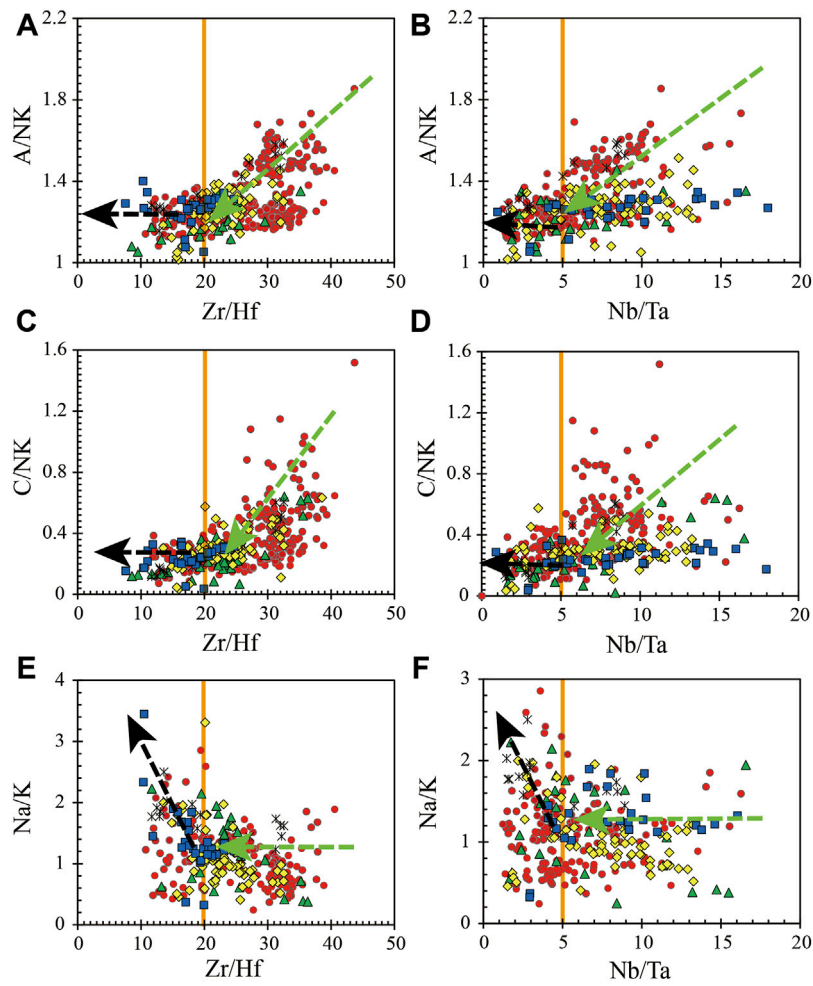


**FIGURE 5**  
 Relationship between the textural change in the silica melts (represented by A/NK, C/NK, and Na/K) and high-field strength elements' ratios (Zr/Hf and Nb/Ta).  $A/NK = Al_2O_3 / (Na_2O + K_2O)$ ,  $C/NK = CaO / (Na_2O + K_2O)$ ,  $Na/K = Na_2O / K_2O$

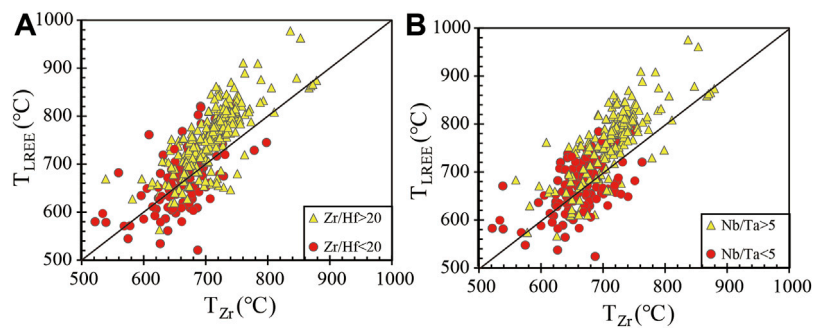


**FIGURE 6**  
 Zircon saturation thermometry  $T_{Zr}$  vs monazite saturation thermometry  $T_{LREE}$  in the high-silica magmas.

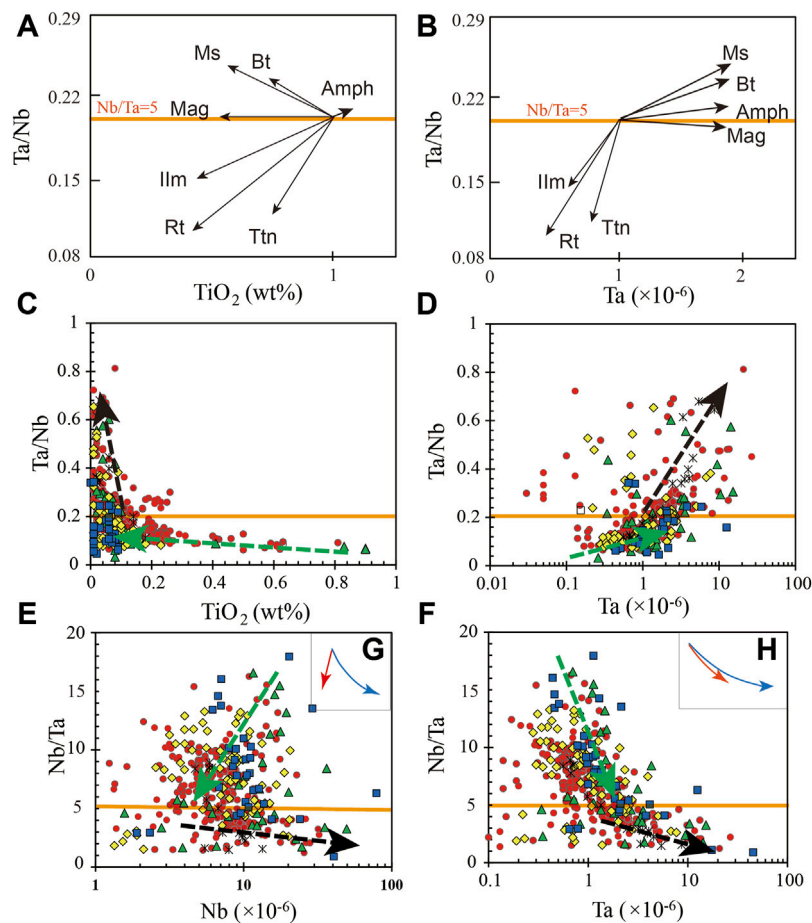


**FIGURE 7**

Nb and Ta compositional evolution in granites with fractionation of the Ti-bearing oxides (rutile, titanite, and ilmenite) and mica (biotite and muscovite). (A,B) are models from Stepanov et al. (2014); (G,H) are models from Ballourd et al. (2016). Black arrow represents fractionation of micas which produces increase in Ta and Nb contents and Ta/Nb. Green arrow represents fractionation of assemblage made of Ti-bearing oxides and mica which produces a decrease in Nb contents but a slightly increase in Ta contents and Ta/Nb.

Ta (Linnen and Keppler, 1997). Recently, Stepanov et al. (2014) proposed that biotite and muscovite may be important minerals that are able to fractionate Ta from Nb. Additionally, Ballourd et al. (2016) suggested that Nb and Ta could be fractionated in evolved peraluminous granites during the interaction with late magmatic fluids. Similar to Zr-Hf, Nb-Nb/Ta and Ta-Nb/Ta systematic relationships are complex in the Himalayan Miocene leucogranites. In the high-silica peraluminous magma, when the melt's Nb/Ta ratio passes approximately 5, the relationship between Nb (or Ta) and Nb/Ta ratios also changes. As the Nb/Ta ratio decreases, Nb first decreases and then increases (Figure 3C). However, Ta first increases slowly and then drastically increases (Figure 3D). Stepanov et al. (2014) modeled the compositional evolution of granites with fractionation of the principal minerals that host Ti, Nb, and Ta (Figures 7A,B). Crystallization of Ti-bearing oxides (rutile, titanite, and ilmenite) decreases the Ti content and Ta/Nb in the melts; biotite and muscovite fractionation significantly

increase Ta/Nb and decreases Ti content in the melt. Ballourd et al. (2016) modeled the evolution of Nb and Ta in liquid  $L_0$  (Nb = 12 ppm, Ta = 1.5 ppm, Nb/Ta = 8) during the fractionation of an assemblage (blue line, Figure 7G) comprising 10 wt% biotite +10 wt% muscovite +80 wt% (quartz + feldspar) and fractionation of an assemblage (red line, Figure 7H) composed of 10 wt% biotite +10 wt% muscovite +.5 wt% ilmenite +79.5 wt% (quartz + feldspar). The different trends observed in the Himalayan granites were an obviously increase in Ta and Nb contents and Ta/Nb produced by fractionation of micas (black arrow) or a decrease in Nb contents but a slightly increase in Ta contents and Ta/Nb produced by fractionation of Ti-bearing oxides and mica (green arrow, Figures 7C,D). Accordingly, we suggest that in the Himalayan Miocene leucogranites, as the melt's Nb/Ta ratio was larger than 5, fractional crystallization minerals were Ti-bearing oxides (rutile, titanite, and ilmenite) and mica, causing a decrease in Nb contents but a slightly increase in Ta contents. As the melt's Nb/Ta ratio passes

approximately 5, at the magmatic-hydrothermal interaction stage, fractional crystallization of biotite and muscovite could not account for the increase in Nb as well as Ta, but decrease in Ti contents. Instead, changes in the relative solubilities of Nb versus Ta (Linnen and Keppler, 1997; Zraïsky et al., 2010) better explain such a pattern due to structure changes in the evolved melts. In addition, in all the systems, the cations of high-field strength elements show a preference for the more depolymerized structural units (Mysen et al., 1982). Experimental studies have shown that the solubility of Nb and Ta in granitic melts increases with an increase in the aluminum saturation index (ASI), a parameter related to the degree of polymerization of the melt (Linnen and Keppler, 1997). Accordingly, as Nb/Ta value pass 5, at the magmatic-hydrothermal interaction stage, the degree of polymerization of the melt decrease. Melt structure change promote increase of mineral solubility, which increase Nb and Ta content but decrease Nb/Ta ratios. Therefore, we propose that the decrease in the Zr/Hf and Nb/Ta ratios in fractionated high-silica peraluminous melts is a consequence of fractional crystallization, sub-solidus hydrothermal alteration and silicate melt structure changes.

## 4.2 Structural changes in the silicate melt

How do molten silicates crystallize? How do they move? Questions such as these underpin many practical problems, ranging from the formation mechanisms of igneous rocks and the dynamics of silicate migration to the mineralization of granites. To address such questions, knowledge of the physical properties of the melt, such as density and viscosity, is necessary. These properties, in turn, are ultimately governed by the melt composition and, therefore, melt structure (Mysen and Richet, 2019; Losq et al., 2021). Studies have proven that melt structure is restricted by its composition (Mysen et al., 1980; Mysen et al., 1982; Zhu and Zhang, 1996). Therefore, the melt structure of various magmas can be determined directly by their geochemical parameters, such as NBO/T (Mysen et al., 1983), M/F (Hou et al., 1992), A/CNK (Linnen and Keppler, 1997), and Na/K (Losq et al., 2021) ratios.

The above discussion suggests that the shift in the Zr-Hf and Nb-Ta systematic relationship is accompanied by important changes in silicate melt structure. Indeed, the geochemical and structural parameters, NBO/T, M/F, and A/CNK, vary with changes in the solubility of high-field strength elements and show similar trends (Figure 4). As the melt's Zr/Hf ratio passes approximately 20 or Nb/Ta ratio passes approximately 5, NBO/T, M/F, and A/CNK, vary from decreasing to increasing. Therefore, it is inferred that the polymerization of the melts first increases and then decreases. Losq et al. (2021) proposed i-Melt, a model integrating a feed-forward neural network and physical equations, which was developed to predict alkali aluminosilicate melt and glass properties, including configurational entropy, glass transition temperature, fragility,

viscosity, density, optical refractive index, and Raman spectra. In i-Melt model, the calculated NBO/T increases significantly in peralkaline melts as the (Na+K)/Al ratio increases above 1. Meanwhile, NBO/T also show apparently change as the (Na+K)/Al ratio are less than 1, and NBO/T increases significantly as (Na+K)/Al ratios are between .83–.90. The variation of NBO/T testify the depolymerization of the melt or structure changes of the melt. In the Himalayan high-silica peraluminous granites, A/NK and C/NK vary from decreasing to constant, but Na/K varies from constant to increasing (Figure 5). As the melt's Zr/Hf ratio passes approximately 20 or Nb/Ta ratio passes approximately 5, A/NK decrease to constant value of ~1.2, and NBO/T increases (Figures 4A,B). Above observations are supported by the i-Melt model. The structural and composition variations observable in Figures 3–5 are associated with very important changes in the physical and chemical properties of the melt. Di Genova et al. (2017) shown that eruptions of silicic volcanoes were found to be more explosive when the rhyolite melt is rich in K and Al. Furthermore, the compositions of silicic lavas form two clusters associated with effusive and explosive eruptions, when viewed in terms of the rheological apgaitic index K/(K+Na) ratios (Di Genova et al., 2017). Losq et al. (2021) observed that K-rich melts have systematically different structures and higher viscosities compared to Na-rich melts and proved that the structural and thermodynamic variations are associated with very important changes in term of melt viscosity. Accordingly, the compositional changes behind the trends shown in Figure 3 are accompanied by changes in melt's structure and viscosity. As the Zr/Hf and Nb/Ta ratios of the melt pass approximately 20 and 5, respectively, structural changes in silicate melt lead to a decrease in granitic viscosity, which in turn promotes extensive fractional crystallization of granitic melts.

## 4.3 Influence of the changes in the silicate melt structure on the enrichment of rare elements

Many Himalayan leucogranites have been identified as highly fractionated granites that contain rare-metal minerals, such as beryl and chrysoberyl; columbite-tantalite, tapiolite, and pyrochlore-microlite; rutile and fergusonite; and zinnwaldite, lepidolite, spodumene, and petalite (Wu et al., 2020; Qin et al., 2021). Therefore, the Himalayan leucogranites have a high potential to produce deposits of economically relevant rare metals (e.g., Be, Li, W, Sn, Nb, and Ta) (Wang et al., 2017; Zeng and Gao, 2017; Qin et al., 2021; Wu et al., 2021).

Ballour et al. (2016) suggested that an Nb/Ta ratio of ~5 and an Nb/Ta ratio of ~18 may be good markers to discriminate mineralized granites from barren peraluminous granites. Furthermore, Zr-Zr/Hf and Hf-Zr/Hf complex systematic relationship in the Himalayan leucogranites imply that the silicate melt structure will change as Zr/Hf ratio passes

approximately 20 and Nb/Ta ratio passes 5. Therefore, we propose that the change in the silicate melt structure is an important factor in the mineralization of economically relevant rare elements.

## 5 Conclusion

- (1) Most Himalayan Cenozoic leucogranites are peraluminous high-silica magmas, which have experienced extensive fractional crystallization.
- (2) The Zr-Hf and Nb-Ta systematic relationships are complex in the Himalayan Miocene leucogranites.
- (3) As the melt's Zr/Hf and Nb/Ta ratios exceed 20 and 5, respectively, the silicate melt structure changes.
- (4) The change in melt structure could be characterized geochemical parameters: NBO/T, M/F, A/CNK, A/NK, C/NK, and Na/K.
- (5) The change in melt structure leads to a decrease in granitic viscosity, which in turn promotes extensive fractional crystallization of granitic melts and mineralization of economically relevant rare elements in the Himalayan Cenozoic leucogranites.

## Data availability statement

The original contributions presented in the study are included in the article/Supplementary Material, further inquiries can be directed to the corresponding author.

## Author contributions

L-EG: conceptualization, funding acquisition, investigation, and writing—original draft. LZ: conceptualization, funding

## References

- Aikman, A. B., Harrison, T. M., and Ding, L. (2008). Evidence for early (>44 Ma) Himalayan crustal thickening, Tethyan Himalaya, southeastern Tibet. *Earth Planet. Sci. Lett.* 274 (1–2), 14–23. doi:10.1016/j.epsl.2008.06.038
- Ballouard, C., Poujol, M., Boulvais, P., Branquet, Y., Tartese, R., and Vignerresse, J. (2016). Nb-Ta fractionation in peraluminous granites: A marker of the magmatic-hydrothermal transition. *Geology* 44, 231–234. doi:10.1130/g37475.1
- Bottinga, Y., and Richet, P. (1996). Silicate melt structural relaxation: Rheology, kinetics, and Adam-Gibbs theory. *Chem. Geol.* 128, 129–141. doi:10.1016/0009-2541(95)00168-9
- Chen, X. L., and Gao, S. (1986). Improvement of calculation method of melt depolymerization parameter NBO/T value and its application. *Geol. Sci. Technol. Inf.* 5 (2), 131–136.
- Crisp, L. J., and Berry, A. J. (2022). A new model for zircon saturation in silicate melts. *Contrib. Mineral. Pet.* 177, 71. doi:10.1007/s00410-022-01925-6
- Di Genova, D., Kolzenburg, S., Wiesmaie, S., Dallanave, E., Neuville, D. R., Hess, K. U., et al. (2017). A compositional tipping point governing the mobilization and eruption style of rhyolitic magma. *Nature* 552, 235–238. doi:10.1038/nature24488
- Dickenson, M. P., and Hess, P. C. (1982). Redox equilibria and the structural role of iron in aluminosilicate melts. *Contrib. Mineral. Pet.* 78, 352–357. doi:10.1007/bf00398931
- Dostal, J., Kontak, D. J., Gerel, O., Shellnutt, J. G., and Fayek, M. (2015). Cretaceous ongonites (topaz-bearing albite-rich microleucogranites). From ongon khairkhan, Central Mongolia: Products of extreme magmatic fractionation and pervasive metasomatic fluid: Rock interaction. *Lithos* 236–237, 173–189. doi:10.1016/j.lithos.2015.08.003
- Gao, L. E., Zeng, L. S., and Asimow, P. D. (2017). Contrasting geochemical signatures of fluid absent versus fluid-fluxed melting of muscovite in metasedimentary sources: The Himalayan leucogranites. *Geology* 45 (1), 39–42. doi:10.1130/g38336.1
- Gao, L. E., and Zeng, L. S. (2014). Fluxed melting of metapelite and the formation of Miocene high-CaO two-mica granites in the Malashan gneiss dome, southern Tibet. *Geochim. Cosmochim. Acta* 130, 136–155. doi:10.1016/j.gca.2014.01.003
- Gao, L. E., Zeng, L. S., Gao, J. H., Zhao, L. H., JiaHao, G., and LingHao, Z. (2021b). Enrichment mechanisms of Sn-Cs-Tl in the Himalaya leucogranite. *Acta Petrol. Sin.* 37 (10), 2923–2943. doi:10.18654/1000-0569/2021.10.01

acquisition, writing—review, and editing. LZ, LY, and YW: Discussion, Investigation.

## Funding

This work was supported by the National Science Foundation of China (Grant Numbers 41873023 and 92055202), the Second Tibetan Plateau Scientific Expedition and Research (Grant Number 2019QZKK0702), National Key Research and Development Plan (Grant Number 2021YFC2901901), and China Geological Survey (Grant DD20221817&DD20221630).

## Conflict of interest

The authors declare that the research was conducted in the absence of any commercial or financial relationships that could be construed as a potential conflict of interest.

## Publisher's note

All claims expressed in this article are solely those of the authors and do not necessarily represent those of their affiliated organizations, or those of the publisher, the editors and the reviewers. Any product that may be evaluated in this article, or claim that may be made by its manufacturer, is not guaranteed or endorsed by the publisher.

## Supplementary material

The Supplementary Material for this article can be found online at: <https://www.frontiersin.org/articles/10.3389/feart.2022.1097537/full#supplementary-material>

- Gao, L. E., Zeng, L. S., Hu, G. Y., Wang, Y. Y., Wang, Q., Guo, C. L., et al. (2019). Early Paleozoic magmatism along the northern margin of East Gondwana. *Lithos* 334–335, 25–41.
- Gao, L. E., Zeng, L. S., Zhao, L. H., Hou, K. J., Guo, C. L., Gao, J. H., et al. (2021a). Geochemical behavior of rare metals and high field strength elements during granitic magma differentiation: A record from the Borong and Malashan gneiss domes, Tethyan Himalaya, southern Tibet. *Lithos* 398399, 106344. doi:10.1016/j.lithos.2021.106344–
- Guo, C. L., Zeng, L. S., Gao, L. E., Su, H. Z., Ma, X. H., and Yin, B. (2017). Highly fractionated granitic minerals and whole-rock geochemistry prospecting markers in Hetian, Fujian Province. *Acta Geol. Sin.* 91 (8), 1796–1817.
- Hodges, K. V. (2000). Tectonics of the Himalaya and southern Tibet from two perspectives. *Geol. Soc. Am. Bull.* 112, 324–350. doi:10.1130/0016-7606(2000)112<324:tothas>2.0.co;2
- Hou, Z. Q. (1992). Magma chemistry, melt structure and phosphorus potential of the P-rich (potassic) alkaine complexes in some areas of northern China. *Acta Geol. Sin.* 8 (3), 222–233.
- King, J., Harris, N., Argles, T., Parrish, R., and Zhang, H. F. (2011). Contribution of crustal anatexis to the tectonic evolution of Indian crust beneath southern Tibet. *Geol. Soc. Am. Bull.* 123, 218–239. doi:10.1130/b30085.1
- Linnen, R. L., and Keppler, H. (1997). Columbite solubility in granitic melts: Consequences for the enrichment and fractionation of Nb and Ta in the Earth's crust. *Contrib. Mineral. Petrol.* 128 (2), 213–227. doi:10.1007/s004100050304
- Linnen, R. L., and Keppler, H. (2002). Melt composition control of Zr/Hf fractionation in magmatic processes. *Geochim. Cosmochim. Acta* 66 (18), 3293–3301. doi:10.1016/s0016-7037(02)00924-9
- Liu, Z. C., Wu, F. Y., Ji, W. Q., Wang, J. G., and Liu, C. Z. (2014). Petrogenesis of the Ramba leucogranite in the Tethyan Himalaya and constraints on the channel flow model. *Lithos* 208–209, 118–136. doi:10.1016/j.lithos.2014.08.022
- Liu, Z. C., Wu, F. Y., Liu, X. C., Wang, J. G., Yin, R., Qiu, Z. L., et al. (2019). Mineralogical evidence for fractionation processes in the Himalayan leucogranites of the Ramba Dome, southern Tibet. *Lithos* 340–341, 71–86. doi:10.1016/j.lithos.2019.05.004
- Losq, C. L., Valentine, A., Mysen, B. O., and Neuvile, D. R. (2021). Structure and properties of alkali aluminosilicate glasses and melts: Insights from deep learning. *Geochim. Cosmochim. Acta* 314 (1), 27–54. doi:10.1016/j.gca.2021.08.023
- Mo, X. X. (1985). Magmatic melt structure. *Geol. Sci. Technol. Inf.* 4 (2), 21–1.
- Montel, J. M. (1993). A model for monazite/melt equilibrium and application to the generation of granitic magmas. *Chem. Geol.* 110, 127–146. doi:10.1016/0009-2541(93)90250-m
- Mysen, B. O., and Richet, P. (2019). *Silicate Glasses and melts*. Amsterdam, Netherlands: Elsevier Science. doi:10.1016/C2018-0-00864-6
- Mysen, B. O. (1983). The structure of silicate melts. *Annu. Rev. Earth Planet. Sci.* 11, 75–97. doi:10.1146/annurev.ea.11.050183.000451
- Mysen, B. O., Virgo, D., and Scarfe, C. M. (1980). Relations between the anionic structure and viscosity of silicate melts - a Raman spectroscopic study. *Am. Mineral.* 65, 690–710.
- Mysen, B. O., Virgo, D., and Seifert, F. A. (1982). The structure of silicate melts: Implications for chemical and physical properties of natural magma. *Rev. Geophys.* 20, 353–383. doi:10.1029/rg020i003p00353
- Patino Douce, A. E., and Harris, N. (1998). Experimental constraints on Himalayan anatexis. *J. Pet.* 39, 689–710. doi:10.1093/ptro/39.4.689
- Qin, K. Z., Zhao, J. X., He, C. T., Shi, R. Z., and RuiZhe, S. (2021). Discovery of the Qongjiagang giant lithium pegmatite deposit in Himalaya, Tibet, China. *Acta Petrol. Sin.* 37 (11), 3277–3286. doi:10.18654/1000-0569/2021.11.02
- Stepanov, A. S., and Hermann, J. (2013). Fractionation of Nb and Ta by biotite and phengite: Implications for the “missing Nb paradox”. *Geology* 41, 303–306. doi:10.1130/g33781.1
- Stepanov, A. S., Mavrogenes, J. A., Meffre, S., and David Son, P. (2014). The key role of mica during igneous concentration of tantalum. *Contrib. Mineral. Pet.* 167, 1009–1016. doi:10.1007/s00410-014-1009-3
- Wang, R. C., Wu, F. Y., Xie, L., Liu, X. C., Wang, J. M., Yang, L., et al. (2017b). A preliminary study of rare - metal mineralization in the Himalayan leucogranite belts, south Tibet. *Sci. China - Earth Sci.* 60 (9), 1655–1663. doi:10.1007/s11430-017-9075-8
- Wang, Y. H., Zeng, L. S., Gao, L. E., Guo, C. L., Hou, K. J., Zhang, L. F., et al. (2017a). Neoproterozoic magmatism in eastern Himalayan terrane. *Chin. Sci. Bull.* 62 (6), 415–424. doi:10.1016/j.scib.2017.02.003
- Watson, E. B., and Harrison, T. M. (1983). Zircon saturation revisited. Temperature and composition effects in a variety of crustal magma types. *Earth Planet. Sci. Lett.* 64, 295–304. doi:10.1016/0012-821x(83)90211-x
- Weinberg, R. F., and Hasalova, P. (2015). Water-fluxed melting of the continental crust: A review. *Lithos* 212–215, 158–188. doi:10.1016/j.lithos.2014.08.021
- Wu, F. Y., Liu, X. C., Liu, Z. C., Wang, R. C., He, S. X., Wang, J. M., et al. (2020). Highly fractionated Himalayan leucogranites and associated rare-metal mineralization. *Lithos* 352 (353), 105319. doi:10.1016/j.lithos.2019.105319
- Wu, F. Y., Liu, Z. C., Liu, X. C., and Ji, W. Q. (2015). Himalayan leucogranite: Petrogenesis and implications to orogenesis and plateau uplift. *Acta Pet. Sin.* 31, 1–36.
- Wu, F. Y., Wang, R. C., Liu, X. C., Xie, L., and Lei, X. (2021). New breakthroughs in the studies of Himalayan rare-metal mineralization. *Acta Pet. Sin.* 37 (11), 3261–3276. doi:10.18654/1000-0569/2021.11.01
- Zaraisky, G. P., Korzhinskaya, V., and Kotova, N. (2010). Experimental studies of Ta<sub>2</sub>O<sub>5</sub> and columbite–tantalite solubility in fluoride solutions from 300 to 550°C and 50 to 100 MPa. *Mineral. Pet.* 99, 287–300. doi:10.1007/s00710-010-0112-z
- Zeng, L. S., and Gao, L. E. (2017). Cenozoic crustal anatexis and the leucogranites in the Himalayan collisional orogenic belt. *Acta Pet. Sin.* 33 (5), 1420–1444.
- Zeng, L. S., Gao, L. E., Xie, K. J., and Liu-Zeng, J. (2011). Mid-eocene high Sr/Y granites in the northern Himalayan gneiss domes: Melting thickened lower continental crust. *Earth Planet. Sci. Lett.* 303, 251–266. doi:10.1016/j.epsl.2011.01.005
- Zhang, J. J., Santosh, M., Wang, X. X., Guo, L., Yang, X. Y., and Zhang, B. (2012). Tectonics of the northern Himalaya since the India–Asia collision. *Gondwana Res.* 21 (4), 939–960. doi:10.1016/j.gr.2011.11.004
- Zhang, H. F., Harris, N., Parrish, R., Kelley, S., Zhang, L., Rogers, N., et al. (2004). Causes and consequences of protracted melting of the mid-crust exposed in the North Himalayan antiform. *Earth Planet. Sci. Lett.* 228 228, 195–212. doi:10.1016/j.epsl.2004.09.031
- Zhu, Y. F., and Zhang, C. Q. (1996). *Silicate melt structure*. Beijing: Geological Publishing House.